Studies Related to In-Plane Flow Behavior of Elastomer Matrix in Nonwoven Fibrous Structures

M. EPSTEIN[1,*] and R. L. SHISHOO[2]

[1]Technical Research Centre of Finland, Laboratory for Plastics and Fibre Technology, Tampere, Finland; and
[2]Chalmers University of Technology/TEFO, Gothenburg, Sweden

SYNOPSIS

The purpose of the present work has been to produce knowledge as regards the rheological behavior of polymer matrix in nonwoven fibrous reinforcing structures for composites. The results are expected to contribute toward a better understanding of flow mechanisms in fibrous systems in order to develop better techniques for fabricating elastomer-based composites. Theoretical and experimental analyses have been made of interactions between the structural parameters of the fibrous mats and the flow characteristics of the matrix with systematically varied material and process parameters. In nonwoven mats with fibers laid lengthwise, the flow rate along the fiber direction was found to be significantly higher than the flow rate crosswise to the fiber direction. Nonwoven mats with multidirectionally laid fibers exhibited a practically radial flow front pattern. Nonwoven mats made of coarser fibers showed greater matrix polymer flow rate as compared with finer fibers. The matrix flow distance was proportional to the logarithm of injection time. The decrease of pressure in the mold cavity was linearly proportional to the matrix flow distance. The dependence of permeability on the level of compression of the fibrous structure is in agreement with the results published by other workers. © 1994 John Wiley & Sons, Inc.

INTRODUCTION

Structural reaction injection molding (SRIM) is usually used to produce stiff composites containing polyester or epoxy matrices. The fiber-reinforcement structure in the form of mats or fabrics are placed into the cavity of a mold prior to applying vacuum, followed by injecting the two-component polymer. Pressure, sometimes in combination with vacuum, is used to introduce the polymer into the mold cavity and to force it to penetrate the fiber-reinforcement structure and form the polymer matrix. For elastomer composite formation, this molding concept is new.[1-3] Data on flow through composite reinforcements using reactive elastomer fluids are virtually nonexistent in the literature. One major drawback in the fiber reinforcement of rubber-based elastomer composites has been the difficulty in introducing fibers of a length larger than only a few millimeters in randomly dispersed directions into the matrix.[4] Epstein and Shishoo described new methods to fabricate flat samples of fiber-reinforced elastomer composites with three-dimensional fiber structures in the fiber reinforcement.[5,6] They also reported measurements of the adhesion between an elastomer and different fiber types.[7]

Theoretical Considerations Regarding Fluid Flow in Fibrous Structures

The matrix polymer must quickly fill the cavity of the mold and wet all fibers in the structural reaction injection-molding process. Macosko analyzed the flow in terms of flow of liquid throughout the entire cavity and in terms of penetration into fiber bundles of fiber structures in the cavity. Flow into the fiber bundles takes place by capillary action. The driving force is created by surface tension. By roughly estimating the spaces between the fibers as cylindrical channels, the capillary equation can be used[8]:

* To whom correspondence should be addressed.

Journal of Applied Polymer Science, Vol. 51, 1629-1646 (1994)
 CCC 0021-8995/94/091629-18

$$\Delta p = \left(\frac{4\gamma \cos\theta}{d_f}\right) \tag{1}$$

Tandmor and Gogos devised an equation for the penetration distance into a capillary under constant pressure from the Poisieuille equation and a mass balance[9]:

$$L = \frac{d_f}{4}\left(\frac{\Delta p}{2\mu}\right)^{1/2} t^{1/2} \tag{2}$$

By combining eqs. (1) and (2), it is possible to estimate the distance polymer liquid can travel by capillary action in a fiber bundle:

$$L = (d_f \times t \times \gamma \times \cos\theta/8 \times \mu)^{1/2} \tag{3}$$

which allows estimation of the distance that polymer liquid can travel by capillary action in a fiber bundle. If the fiber diameter is 10 μm, the resin viscosity 200 poise, surface tension 30×10^{-3} Nm^{-1}, and contact angle 35°, the resin will penetrate 40 μm in the first second. In eq. (3), d_f may be replaced with the diameter of the pores in a porous medium.

Macosko concluded that because the cavity is filled with many small fibers the content of the mold can be treated as a porous medium. Because the pores act as many tiny capillary tubes, the fluid moves like a plug in the mold. For a Newtonian liquid, the average velocity (based on the empty channel) in any direction (x) through the fiber bed is proportional to the pressure gradient and the permeability in that direction[8]:

$$v_x = \frac{K_x}{\mu}\frac{dp}{dx} \tag{4}$$

This equation represents Darcy's law; according to Gebart, the flow in a narrow channel follows Darcy's law.[10]

By combining Darcy's law and the law of conservation of mass, Hirt et al. obtained an expression that describes the pseudosteady process of a Newtonian fluid spreading radially in a porous medium[11]:

$$\frac{d(r^2)}{dt} = \frac{2K_r(p_0 - p_r)}{\epsilon\mu}\frac{1}{\ln(r/R_0)} \tag{5}$$

In an experiment consisting of monitoring the radial position of the spreading front as a function of time a plot of $d(r^2)/dt$ vs. $1/\ln(r/R_0)$ yielded a straight line of slope S from which the permeability could be calculated:

$$K = \frac{S\epsilon\mu}{2(p_0 - p_r)} \tag{6}$$

This calculation is only applicable to a Newtonian fluid and an isotropic spreading pattern.[11] Hirt et al. obtained straight lines in plots of the type described above in experiments with samples of spunbonded nonwoven mats of polypropylene and polyester using a Newtonian resin as fluid. A center hole was precut in the mat at the point where the resin was injected.[11] Examples of permeability values reported are in the order of $2\text{–}4 \times 10^{-10}$ m^2 for epoxy resins flowing in spun-bonded polypropylene and polyester nonwovens[11] and $0.3\text{–}4.5 \times 10^{-10}$ m^2 for mats of chopped glass fiber. The permeability increases with increasing resin volume fraction.[8,11]

Greve devised a method to calculate the porosity from a plot of the wetted area vs. the flow time for polymer spreading in a flat cavity of small cavity height. The plot produced a straight line from the slope of which the porosity was calculated when knowing the volume flux of the polymer and the cavity height.[12] In the case of circular spreading of the polymer from one inlet hole, the wetted area can be approximated to be proportional to the squared flow distance.

If viscosity is constant, i.e., no reaction or heat transfer during filling, the flow in a rectangular channel follows the Poiseuille equation and pressure is linearly dependent on the flow front position.[8]

The dependency on the porosity can be fit with Kozeny's equation, which is usually written

$$K_x = \frac{d_f^2\epsilon^3}{C(1-\epsilon)^2} \tag{7}$$

where good fit has been achieved in experiments with fiber mats using $C = 180$.[8]

Macosko applied Darcy's law to the case of prediction of the time to fill a disk-shaped mold with a part diameter of $2R$ and an inlet diameter of R_0, arriving at the following equation[8]:

$$t = \frac{\mu}{K_r\Delta p}\left\{R^2\ln\frac{R}{R_0} - \frac{R^2 - R_0^2}{2}\right\} \tag{8}$$

Numerous other suggestions have been made to model the polymer flow through fibrous structures based on information of data about the fibrous structure, e.g., permeability, and data about the polymer, e.g., viscosity and pressure. Many of them applied finite element method (FEM) analysis of the data.[13–15] In the majority of reports, the models have been verified using fluids of constant viscosity

during the flow time. The fluids include motor oil,[13] silicon oil,[14] and corn syrup.[12] Chan and Hwang[15] used epoxy resin in a model that takes into consideration the change of viscosity due to the rate of cure in the polymer. The model was an applied FEM calculation.

The purpose of this work was to produce knowledge as regards the rheological properties of elastomer matrix flow in reinforced structures for composites made of nonwoven fiber structures. The work consists partly of an analysis of existing models for the flow of elastomeric polymer fluids in fibrous structures and partly of an investigation of the validity of the models through experiments with elastomeric polymer fluid in fibrous structures.

EXPERIMENTAL

Test Materials

The fibrous reinforcement used consisted of needle-bonded nonwoven mats listed in Table I. The fibers in the mats were of type Trevira poly(ethylene terephthalate) (PET) from Hoechst, polyethylene (LLDPE) from Neste Oy, and gel-spun high-performance polyethylene Dyneema (HPPE) from DSM.[16–18] Each mat consisted entirely of fibers of one type only.

The matrix polymer consisted of a system (Baytech from Bayer Ag) where the polyol was a polyether compound containing small amounts of tertiary aliphatic amine and a primary aromatic diamine and with an added activator. The isocyanate was a polyether–tolylene diisocyanate (TDI) prepolymer with isocyanate groups.[19] Viscosity measurements according to methods described later were made at different temperatures of polyol and isocyanate separately. Both the polyol and isocyanate components exhibited practically Newtonian behavior at 30 and 60°C. Figure 1 shows the effect of aging of matrix polymer mixtures of isocyanate and polyol in terms of viscosity changes as a function of rotational speed for polyurethane matrices of different ages. The figure illustrates an experiment where the initial temperature of the isocyanate and polyol was 30°C. As seen from the figure, the mixture showed practically Newtonian behavior up to 4 min age, but after longer times, the viscosity behavior became clearly time-dependent. An identical experiment where the initial temperature of the matrix components was 45°C showed similar behavior. Figure 2 shows the effect of temperature of matrix polymer in terms of viscosity change as function of time for different initial temperatures of polyol and isocyanate. The viscosity of the mixtures is indirectly proportional to the initial temperature of the components up to about 60 s after mixing. After about 60 s, the viscosities started to increase, the rate of increase being proportional to the initial temperatures.

Tests were performed to characterize the materials, i.e., the dimensional and mechanical properties of fibers and mats as well as rheological properties of the matrix materials. The process variables during sample fabrication as well as the dimensional properties of the fabricated samples were measured.

The reinforcement fiber mats were weighed after conditioning for 24 h at 65% RH and 20°C. Their thickness was then measured according to standard methods[20,21] at three sites as indicated in Figure 3 using a pressure of 0.5 kPa in the Shirley thickness gauge. The figure shows the outline of the mold cavity; the area inside the outline represents the area of the mat sample used for composite sample fabrication. The thickness of the mat during the experiments is expressed by the term level of compression as percent according to the following equation:

$$c_1 = ((h_s - h_m)/h_s) \times 100 \qquad (9)$$

Table I Fiber Mat Specimens

Mat No.	No. Layers	No. Needling Passes	Fiber Direction[a]	Basis Weight (g/m^2)	Range of Thickness (mm)	Fiber Fineness	
						Type	(dtex)
S1	10	4	l	180	2.8–3.7	PET	1.1
S2	10	4	l	173	3.0–3.8	PET	1.1
S3	10	4	l	200	4.4–5.1	PET	1.7
S4	10	4	l	192	3.3–3.7	PET	1.7
E1	10	2	x	335	3.9–4.5	LLDPE	4.4
E2	10	2	l	313	4.7–4.8	LLDPE	4.4
E3	2	4	l	284	2.9–3.4	HPPE	1.1

[a] l = fibers oriented longitudinally in mat prior to needling; x = fibers oriented multidirectionally in mat.

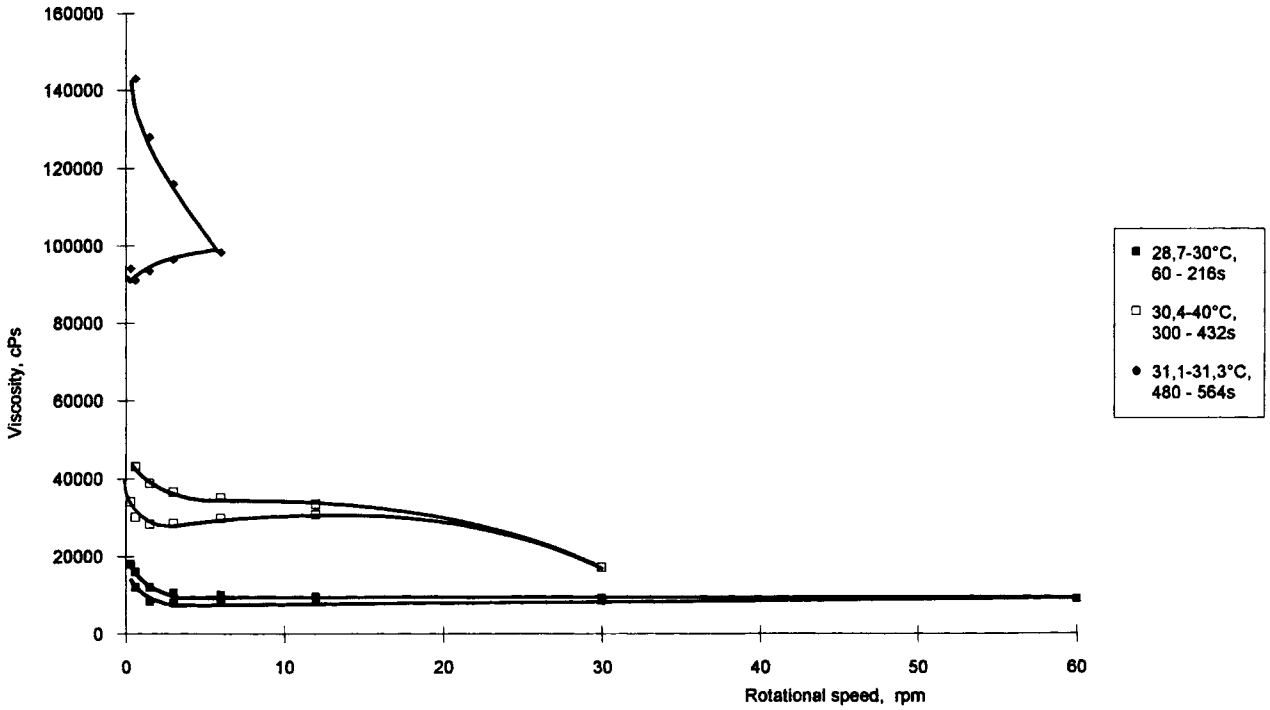

Figure 1 Effect of aging of matrix polymer on viscosity of polyurethane matrices.

The fibrous volume fraction in the mat, as installed in the mold, was calculated using the equation

$$\phi = (w_{ms}/\rho_f)/(a_s \times h_m) \qquad (10)$$

Wicking Characteristics

To characterize the capillary properties of the fiber mats, it was decided to use an index method for test-

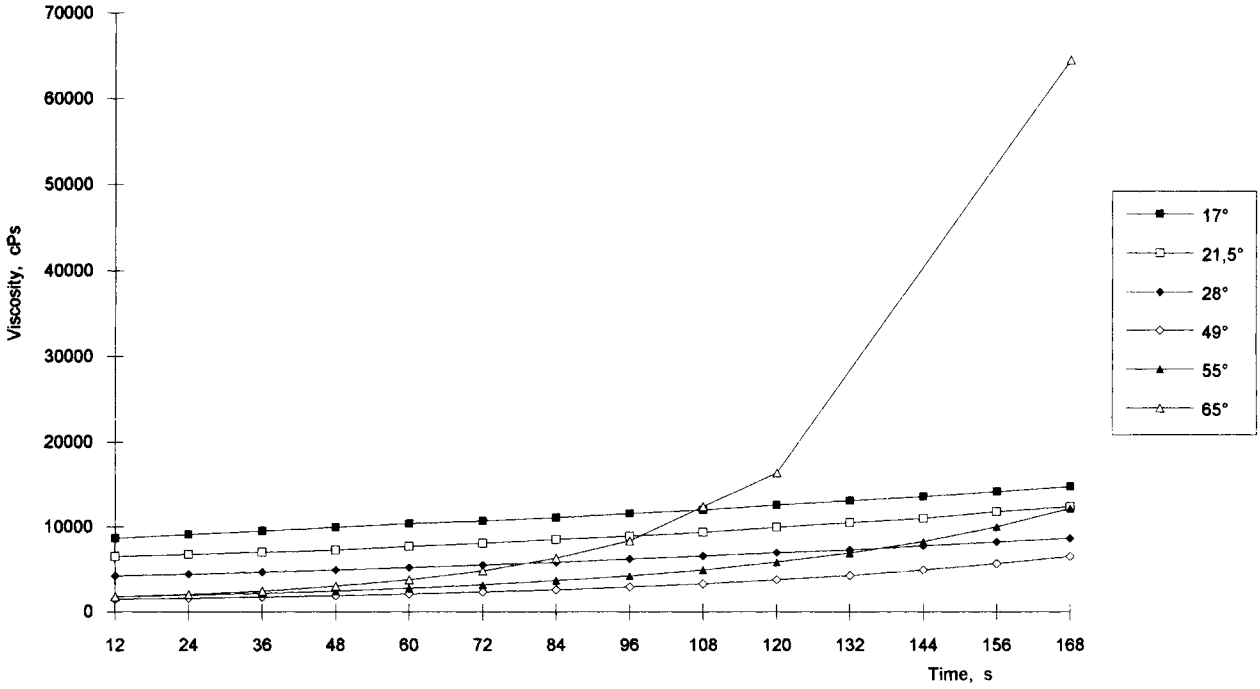

Figure 2 Change in viscosity of matrix polymer. The rate of change of viscosity of polyurethane matrix polymer measured at different initial temperatures of polyol and isocyanate.

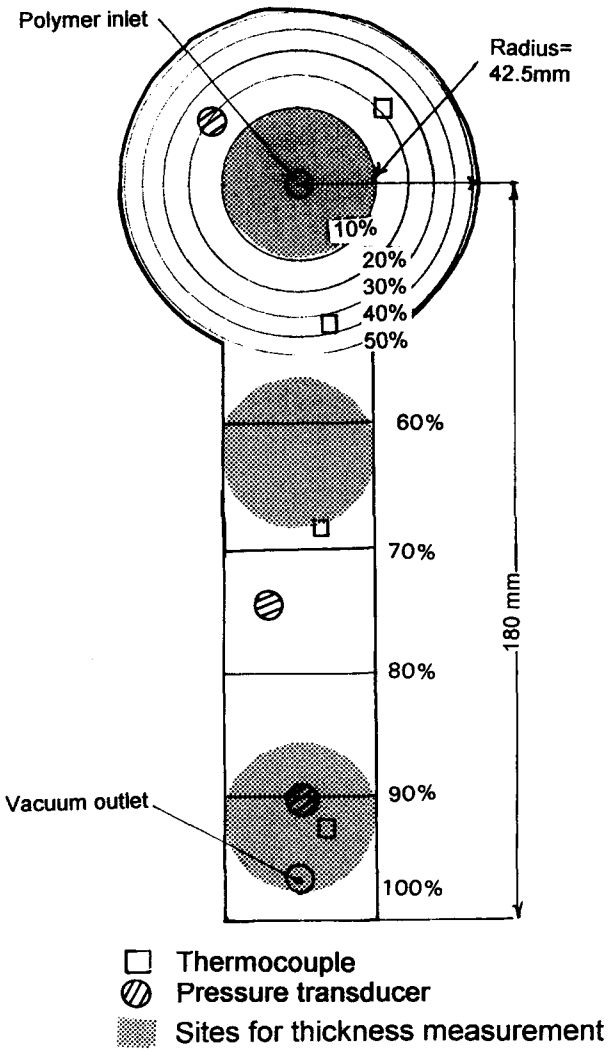

Figure 3 Outline of mold cavity with template for measurement of filling degree superimposed (percent digits represent degree of filling).

ing the wicking properties of mats. It is important to create knowledge of both the fluid flow and the rate of fluid absorption in the wicking process. Wicking in the in-plane direction of the mats at different levels of lateral compression was tested using a modified version of the Swedish standard water absorption test SIS 25 1228 using distilled water as the liquid medium. The test equipment is shown in Figure 4. The fiber mat was sidewise-compressed between two plates, the interdistance being determined by spacer plates of selected caliper. The edge of the mat was adjusted to pertrude 0.5 mm from the clamp edge. The assembly of the plates with the sample was then placed so that the edge of the mat was in contact with the surface of the sintered glass plate. The portion of the sinter surface that was not covered by the assembly was covered by a plastic sheet to prevent water evaporation.

Wicking with elastomer fluid instead of water was tested by installing the fiber mat in the clamp as described above and then placing it over the surface of the elastomer liquid so that the pertruding part of the mat contacted the elastomer. The mat was kept in contact with the elastomer for 10 min; then the mat was removed from the clamps and inspected.

The viscosity of matrix polymer was tested using a Brookfield LVTDV viscometer connected to a Sharp PC6200 computer. The fluid was kept in a vessel isolated by multiple walls or expanded styrofoam during the measurement. The viscosity of the matrix components as well as of the polymer mixtures during polymerization at different temperatures and rotational velocities were measured as function of time.

Description of the Mold and the Fabrication Process

The equipment consisted of a mold, which was the central piece of an assembly for performing the flow-investigation experiments and fabrication of the composites. The other parts of the assembly consisted of the matrix polymer preparation system,

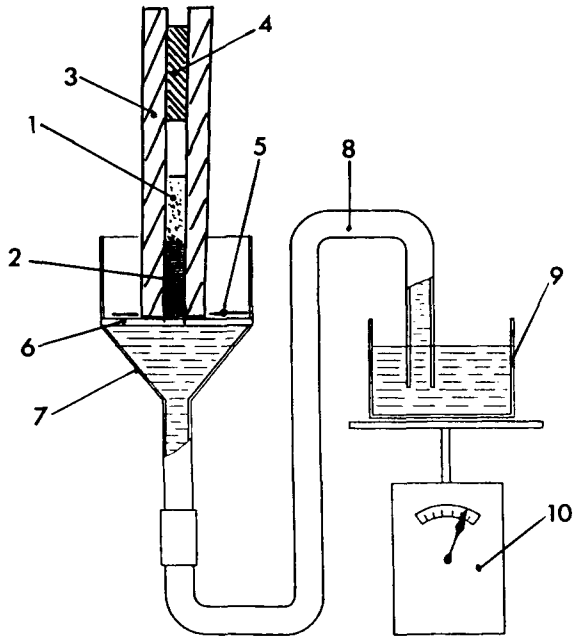

Figure 4 Assembly for measuring vertical wicking in the in-plane direction of mat under sidewise compression: (1) sample; (2) liquid being absorbed; (3) plate; (4) spacer; (5) cover; (6) sintered glass plate; (7) funnel; (8) connection tube; (9) beaker; (10) balance.

controls for temperature and pressure, and the matrix flow monitoring system.

The mold and the assembly of apparatus for monitoring the elastomer flow and fabrication of elastomer composites are basically of the type described earlier by the authors.[6] The important differences are as follows: A mechanical metering and mixing system of type Unipre M 10 was used to meter and mix the isocyanate and polyol and a pressure tank with a pressure regulator was used to provide pressure for the injection of elastomer fluid. An exploded view of the mold is shown in Figure 5. This mold provides an instrument to study the flow characteristics of the elastomer matrix in structural reinforcement molding of elastomer composites and to produce flat composite samples for testing. The new mold differs from the earlier molds used in that it consisted of three plates: top and back plates of laminated toughened glass and a frame plate of rubber sheet. The cavity had only one polymer inlet hole and one vacuum hole, both connected directly to the cavity. Furthermore, the height of the cavity was determined by calibrated spacer plates. The mold was kept in upright position. The outline of the cavity formed a circular part having a radius of 42.5 mm and with the polymer inlet situated in its centerpoint. In this part, circular spreading of the elastomer matrix was studied. A 30 mm-wide portion of the cavity pertruded outward from the circular part; this part allowed fabrication of large enough samples for the testing of mechanical and other properties of composites. The length of the pertrusion was 180 mm from the center of the circle. The height of the cavity, and thereby the thickness of the sample, was determined by the thickness of the spacers (0.5–9 mm). A semipermanent release tape of type Mask-Off was applied to those surfaces of the top and bottom plates that faced the cavity. Both the polymer feed and the vacuum hoses were connected to the mold with nozzles for fast and easy coupling. A data acquisition system with miniature thermocouples and pressure transducers inside the cavity was installed in addition to systems reported earlier by the authors.[6]

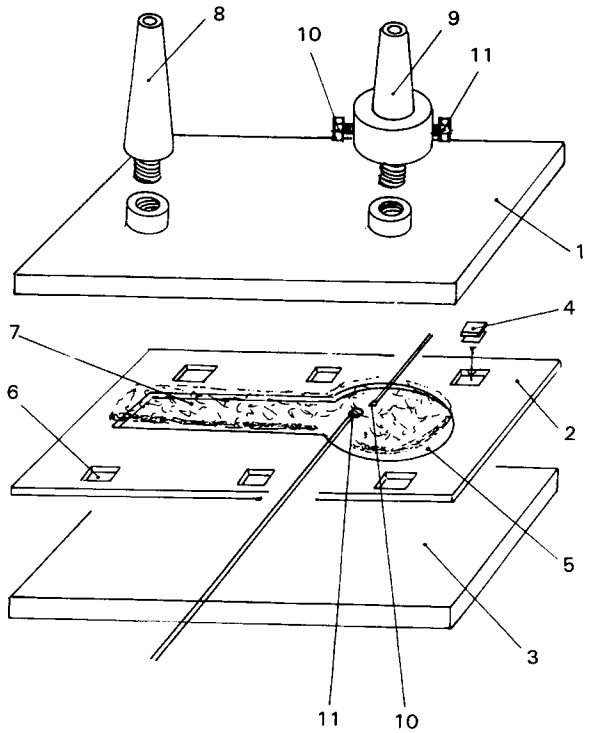

Figure 5 Exploded view of mold: (1) front plate; (2) frame plate; (3) back plate; (4) spacers; (5) cavity; (6) spacer hole; (7) fiber mat; (8) vacuum nozzle; (9) polymer feed nozzle; (10) temperature transducer; (11) thermocouple.

In some experiments, the pressure and temperature variations within the fibrous mats were monitored inside the mold cavity during polymer impregnation, curing, and demolding stages. For that purpose, miniature pressure sensors of type Kyowa PS-A with a diameter of 6 mm and thickness of 0.61 mm and temperature sensors of the PT 100 type were inserted into the interior of the cavity by placing the sensors between the mat and the wall of the cavity. The placement of the individual sensors is shown in Figure 3.

The sample fabrication process consisted of the preparation processes for fiber mats and matrix polymer, the mold assembly, the elastomer-injection process, and the sample demolding.

The preparation process for the fiber mats consisted of opening the fibers on pilot scale fiber opener and carding appropriate amounts of them on a carding machine to form flocks of appropriate dimensions. Mats of 1.1 and 1.7 dtex polyester fibers were produced by laying 10 layers of unidirectionally carded layers of flocks on top of each other with the fibers in the longitudinal direction to give longitudinally laid mats with predominately longitudinally oriented fibers. Then, they were needled four times, turning the mat upside down between each needling pass. One mat was fabricated of 4.4 dtex polyethylene fibers by the method described above with the difference that only two needling passes were performed. A second mat was made of 4.4 dtex polyethylene fibers by stacking the flock layers on top of each other so that the fibers in every second layer was directed lengthwise and in every second layer crosswise to the direction of the mat to give a mul-

tidirectionally laid mat with multidirectionally oriented fibers. Also, this mat was needled in two passes. Finally, one mat was made of 1.1 dtex high-performance polyethylene fibers by using two layers of preneedled (two needling passes) flocks with their fibers directed in the longitudinal direction. The flocks were needled in two passes with intermediate turning, producing a mat with predominately longitudinally oriented fibers. Pieces for making elastomer composite samples were cut with scissors after marking with the aid of a template having the contour and dimensions of the mold cavity. Marks of a tracing color were put on some places of the mat to trace the polymer flow and a grid of lines was printed on the mat surface for the approximation of dislocation of mat during injection molding of composite samples.

At the assembly of the mold, the thickness of the spacer plates was chosen to give the selected height of the cavity [h_m, eq. (9)] and, consequently, the thickness of the sample corresponding to the level of compression selected for the actual experimental conditions. In the experiments that required monitoring of the pressure and temperature in the cavity, the thermocouples and pressure transducers were placed on top of the mat piece. Then, the cavity was closed by putting the top plate on top of the mat piece, frame plate, and spacer plates, and the mold set was clamped with clamps that were tightened until the distance between the top and bottom plates was measured to correspond to the selected value. In experiments requiring heating of the mold, the mold set was placed in an oven until the appropriate temperature was reached and then transferred to the sample fabrication assembly. Experiments were also made with keeping the vacuum hole uppermost as well as with keeping the mold level.

Immediately after mixing, the polymer was transferred via the polymer feed hose to a vessel inside the pressure tank. The polymer-injection procedure was started by connecting the polymer feed hose to the polymer feed nozzle and then the air pressure in the pressure tank was raised to preset pressure and polymer flow into the cavity started. Thus, the most recently mixed polymer first entered the mold; the time sequence from the end of mixing to the start of injection was 0.5–1 min. At the first sight of the polymer entering the cavity, the vacuum pump was started. This sequence guaranteed that no cold air was sucked through the mat and cooling it before the entry of polymer. The injection was continued until a complete stop of flow occurred.

The video camera as well as the data acquisition system was started before the polymer feed hose was connected to the feed nozzle. The camera was left on during the whole injection sequence. The data acquisition system was left on all the time through the injection sequence and restarted to monitor the demolding procedure.

After the matrix had cured enough to permit safe demolding, the clamps were loosened and removed and the back plate removed. Then, the sample was removed from the cavity and finished by cutting the sprues even with the surface of the sample and removing the burr when appropriate. The fabricated elastomer composite sample was then tested for thickness by measuring wherever appropriate with a Mitutoyo Digimatic Caliper or with a micrometer on the sites indicated in Figure 1 and for weight by weighing the entire sample piece. To investigate whether the flow was pluglike, a cut was made in the sample perpendicular to the flow front and the profile of the front was inspected. The degree of filling was approximated by first measuring the proportion of the surface of the flat part of the sample that was impregnated by polymer using a graded template on the actual sample as shown in Figure 1. The percent values represent a polymer-filled area relative to total area of sample mat; a pluglike flow was assumed. Then, the ratio fiber/total composite, on a weight-on-weight and volume-on-volume basis, was calculated using the following equations:

$$(w/w)_{\text{fib}} = w_{\text{fib}}/(w_{\text{fib}} + w_{\text{matrix}}) \tag{11}$$

when

$$w_{\text{fib}} = a_{\text{sample}}(\alpha/100) \times bw_{\text{mat}} \tag{12}$$

and

$$w_{\text{matrix}} = w_{\text{sample}} - (a_{\text{sample}} \times bw_{\text{mat}}) \tag{13}$$

and

$$\phi = (w_{\text{fib}}/\rho_{\text{fib}})/\{(w_{\text{matrix}}/\rho_{\text{matrix}}) + (w_{\text{fib}}/\rho_{\text{fib}})\} \tag{14}$$

RESULTS AND DISCUSSION

Analyses have been made of various interactions between the structural parameters of the fiber assembly, on the one hand, and the flow characteristics of the matrix, on the other. The parameters studied include the basis weight and thickness as well as the in-plane wicking for the fiber mats. Also, the volume fraction of fibers in mats of different degrees of

compression were estimated. The viscosity of the polyurethane elastomer matrices of various temperatures and ages of the elastomer were analyzed. Some important process and material parameters were studied, e.g., the polymer flow as a function of time, level of compression, fiber types, temperature, injection pressure, and age of polymer as well as combinations of these.

Figure 6 shows the relationship of the fiber volume fraction in 1.1 and 1.7 dtex polyester mats at various levels of compression from 0 to 90% as calculated according to eq. (10). It is obvious that the fiber volume fraction inclines rapidly for compression levels of 70% and upward.

The capillary water absorption through wicking in the in-plane direction of polyester mats made up to different fiber volume fractions is shown in Figure 7. The rate of liquid absorption is rather high for all levels of compression up to 100 s, then the rate becomes lower so that the flow rate can be divided into two phases. The rates during both phases were practically identical for fiber volume fractions above 0.08 v/v. The higher the fiber volume fraction, the sooner the change in flow rate took place. Figure 8 shows the percentage absorbed water 300 s after the start of the experiments as a function of fiber volume fraction with two nonwoven mats containing 1.1 and 1.7 dtex polyester fibers, respectively. The in-plane wicking test indicated one maximum value for percent absorbed water as function of degree of compression. In this experiment, the mat containing 1.1 dtex polyester fiber exhibited a somewhat larger water-absorption capacity and its maximum of absorption occurred at a somewhat less tight compression than was the case for 1.7 dtex fiber mat. During the wicking experiments, the flow was first noticed to take place in practically all pores of the mat, but when the water reached greater height, only part of the pores filled with water. Wicking experiments were also made using polyurethane elastomer fluid at 30°C and polyester mat of 1.7 dtex fibers at a 25% level of compression. In these experiments, no wicking was observed due to the high viscosity of the polyurethane elastomer fluid; this is in agreement with reports in the literature.[8]

The polyurethane matrix flow in SRIM molding generally took place in two sequences that could clearly be separated from each other. The first sequence involved a rapid flow (6–16 mm/s), followed by the second phase with a slow flow (0.1–0.4 mm/s). Generally, the flow distance during the rapid sequence was much greater than that during the slow sequence.

The nature of the slow realm of the polyurethane flow in SRIM molding was analyzed by comparing measured values for velocity with values calculated

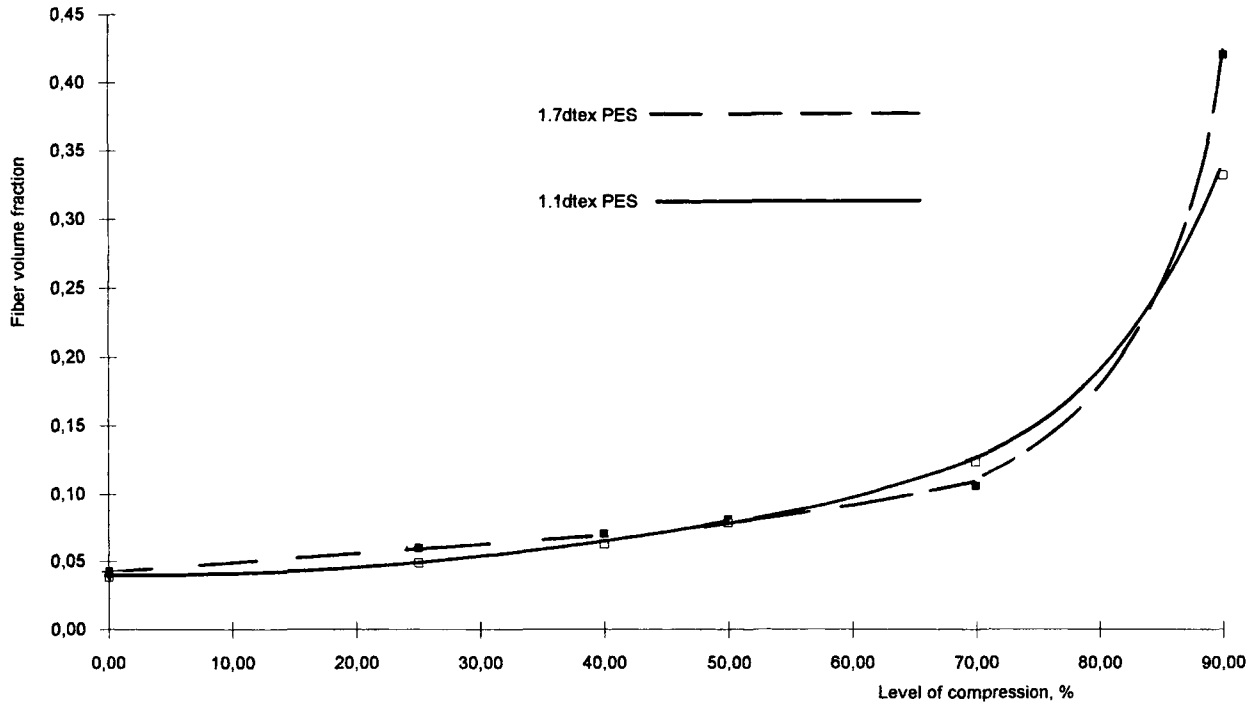

Figure 6 Fiber volume fraction in the mat as function of level of compression, calculated from eq. (10); 1.1 and 1.7 dtex PET fiber mat.

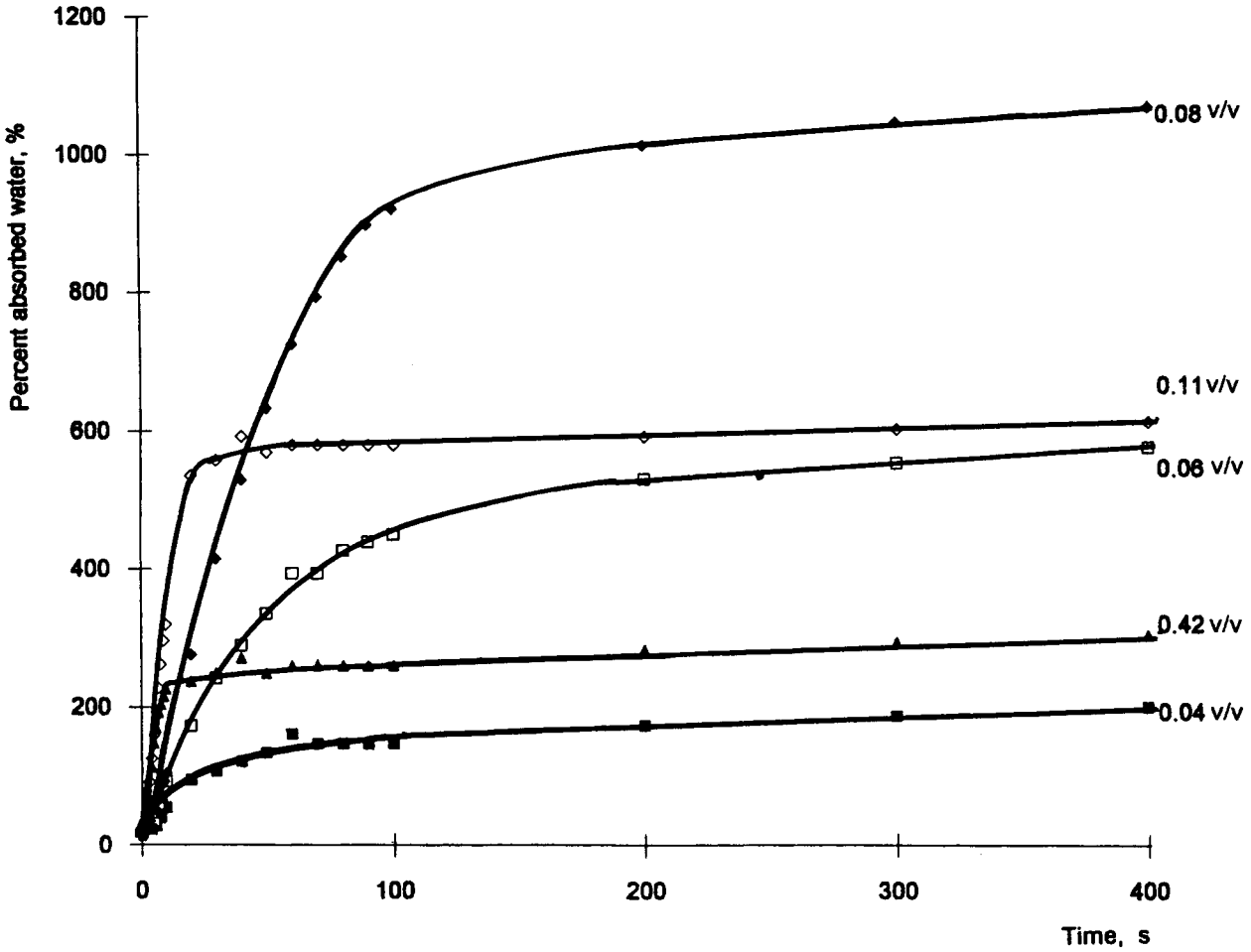

Figure 7 Capillary absorption of water through wicking in the in-plane direction of mat for different fiber volume fractions as function of time (percent absorbed water by weight); 1.7 dtex PET fibers.

with eq. (3). The calculation produced values of the same order of magnitude as those measured for the flow velocity. SEM pictures of a portion of the front that had stopped short of the edge of the fibrous structure showed small menisci of polymer at the roots of fiber ends, as seen in Figure 9. The similarity of velocities as well as the small menisci observed in the SEM picture of the polymer front indicate that the polymer flow in the slow realm may take place by capillary action. The fact that no wicking could be observed when using polymer fluid as the wicking medium contradicts this interpretation of the nature of flow.

The polymer flow front sequences for the SRIM experiments with 1.1 and 4.4 dtex polyethylene fibers are shown in Figure 10, where (A) represents the flow pattern in a mat containing 4.4 dtex; (B), in a mat containing 1.1 dtex fibers predominately in the lengthwise direction of the mold; and (C), in a mat of 4.4 dtex fibers oriented multidirectionally. As seen from the figure, the flow pattern for mats with fibers laid lengthwise have an oval shape with a greater flow rate along the fibers. The flow pattern in the mat of multidirectionally laid fibers is particularly circular. This indicates that the permeability in the direction along the fibers is greater than crosswise to the fibers, which is in agreement with results reported by other workers.[11] The flow rate was greater in the mat fabricated of 4.4 dtex fiber than in the corresponding mat of 1.1 dtex fiber. The rates of polymer flow in the unidirectionally laid mats are shown in Figure 11. The flow rate is about 30% less in the crosswise as compared with lengthwise for mat made up of 4.4 as well as 1.1 dtex fibers. Figure 12 shows the flow rates lengthwise and crosswise for flow in the multidirectionally laid mat. The practically coincident curves support the circular flow pattern observed. In these investigations, only flow

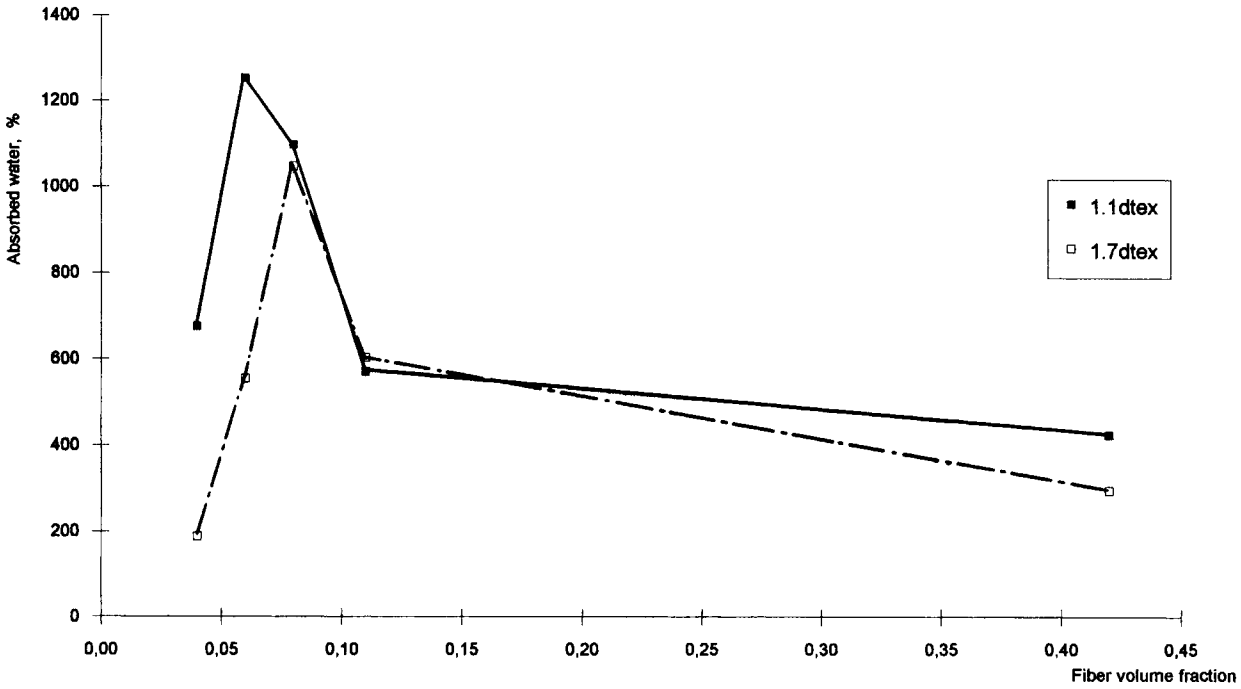

Figure 8 Capillary absorption of water through wicking in the in-plane direction of mat as the function of fiber volume fraction for mats of PET fiber of two different finenesses (percent absorbed water by weight, 300 s after start of absorption).

mechanisms in the in-plane direction of nonwoven mats were studied.

Figure 13 shows elastomer flow rates for mats consisting of different fiber volume fractions made of 1.7 dtex polyester fibers. It can be seen that the flow distance is inversely proportional to the fiber volume fraction. Figure 14 shows the flow distance as function of fiber volume fraction 10 s after the polymer was injected at a pressure of 1 bar into the mats made up of 1.7 dtex polyester fibers. Injection was done at 1 bar pressure. It can be seen that the flow distance decreases with increase in fiber volume fraction, the decrease being more rapid at low volume fractions.

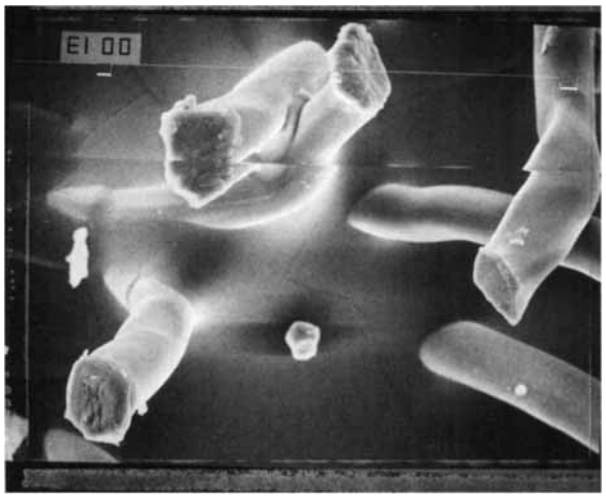

Figure 9 Portion of polymer front with the fiber of the mat sticking out.

Similarity can be noticed in the flow behavior between the wicking experiments using water as the test liquid and the flow experiments using polymer. In both cases, the flow occurs in two phases: an initial rapid followed by a slow phase (Figs. 7 and 11–13). At any certain time after the start of the polymer injection, the flow rate was lower in case of nonwoven mats containing a higher fiber volume fraction. In the wicking experiments, a similar behavior was noticed as regards the amount of absorbed water, which was lower for mats containing higher fiber volume fractions (after having passed a maximum) (Figs. 8 and 14); the flow pattern for the polymer does not show a maximum.

Figure 15 shows a linear relation between flow distance and the logarithm of time for SRIM; the examples represent experiments with different matrix injection pressures. As can be seen, there is a significant increase in the flow rate with increase in pressure for mats containing 0.11 v/v fiber volume fraction.

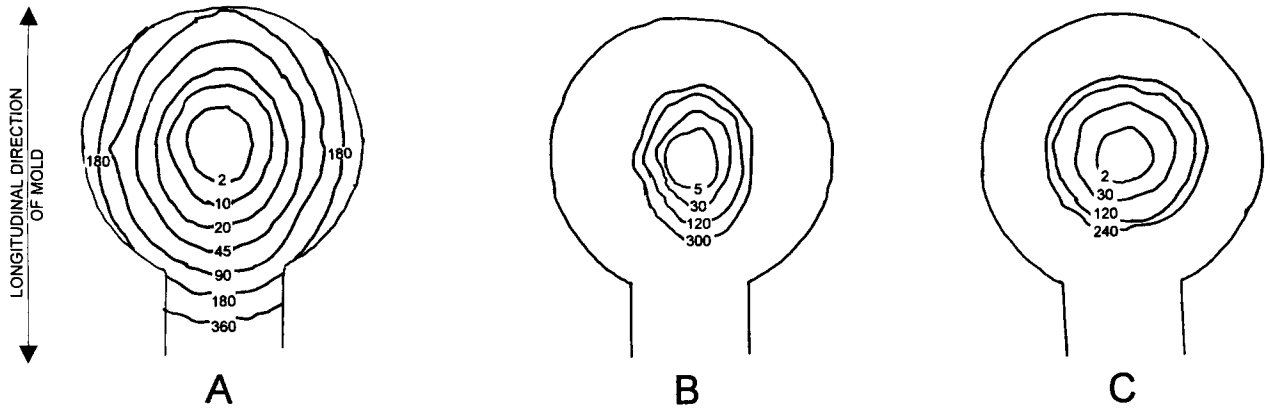

Figure 10 Flow front sequence for matrix flow through nonwoven fabric: (A) unidirectionally laid 4.4 dtex LLDPE; (B) unidirectionally laid 1.1 dtex HPPE (re Fig. 11); (C) multidirectionally laid 4.4 dtex LLDPE (Re. Fig. 11); digits express flow time (s).

The influence of temperature on the rate of matrix flow rate in mats containing 1.1 dtex polyester fibers at two different temperatures is shown in Figure 16. The flow rate increased with increase in temperature regardless of the level of compression and the fiber fineness. This was due to the markedly lower viscosity for polyurethane elastomer at 60°C compared with the viscosity at 30°C, as can be seen from Figure 8. The higher the temperature, the larger is the transition time from the faster realm of flow velocity to a slower one.

A typical example of pressure distribution at different measuring points during the filling of the mold is given in Figure 17. In most cases, the pressure remained unchanged once the equilibrium level was reached. Figure 18 shows plots of pressure vs. flow distance at different levels of initial pressures for mats made of 1.1 dtex polyester fibers and at 25% level of compression. The slope of the curves up to 3.8 bar is practically similar. This is in agreement with the results from experiments using an empty mold reported in the literature.[8]

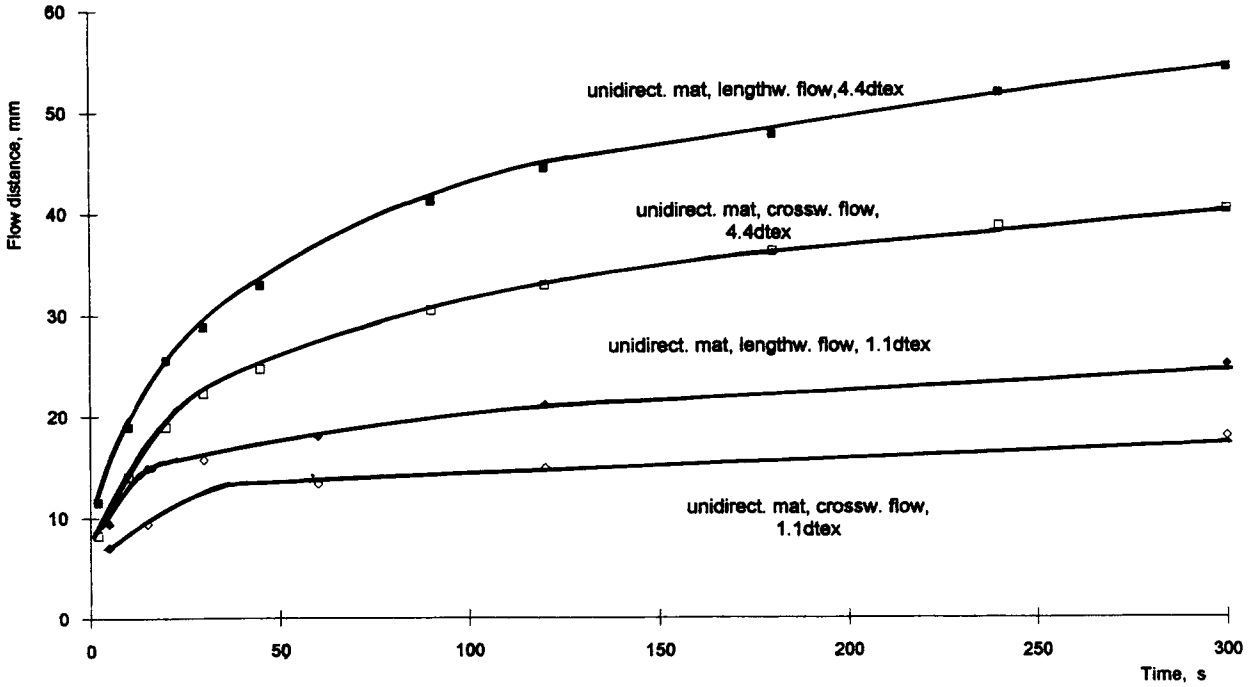

Figure 11 Influence of fiber orientation on the rate of matrix flow, unidirectionally laid mats of 1.1 and 4.4 dtex polyethylene fibers; 2.6 bar; level of compression 50%.

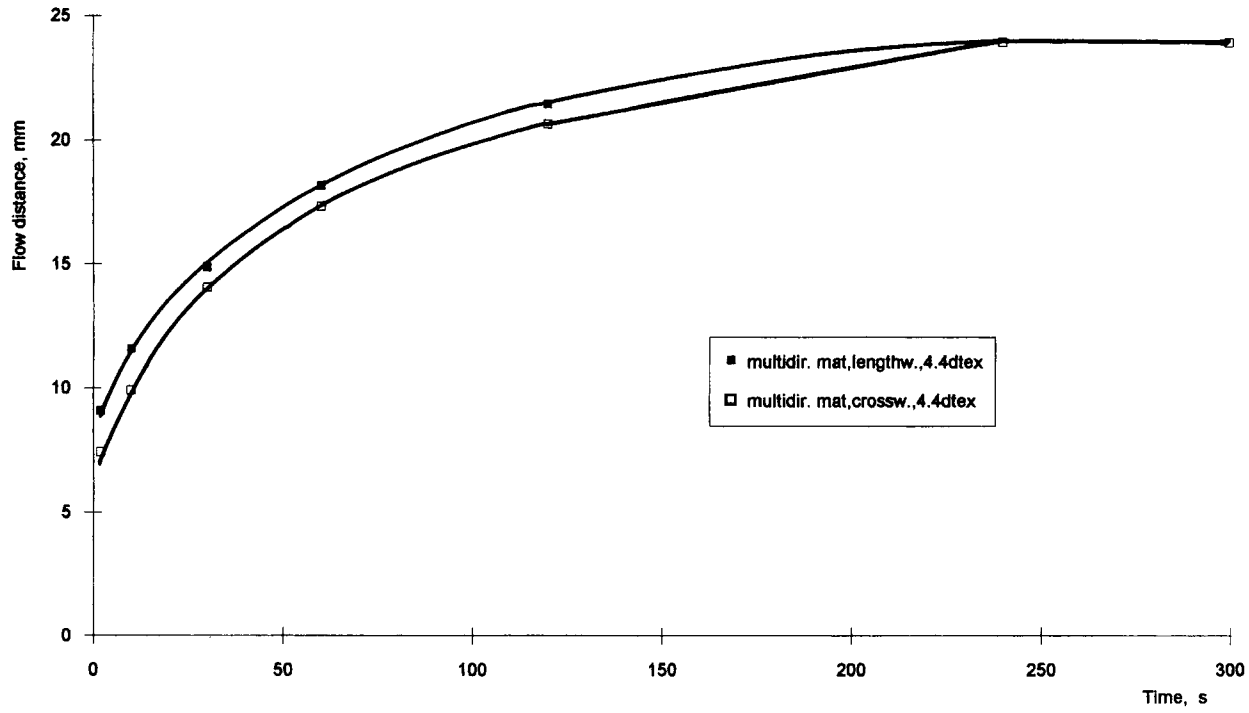

Figure 12 Influence of fiber orientation on the rate of matrix flow, multidirectionally laid mat; 4.4 dtex LLDPE; 2.6 bar; level of compression 50%.

Diagrams plotted according to eq. (5) for obtaining slope S for calculation of permeability showed a linear relationship between $1/\ln(r/R_0)$ and $d(r^2)/dt$ for most of our experiments (Fig. 19). This is in agreement with results of other workers using Newtonian fluids.[11] The values of the permeability of mats made of 1.1 and 1.7 dtex polyester fiber at different levels of compression calculated according to

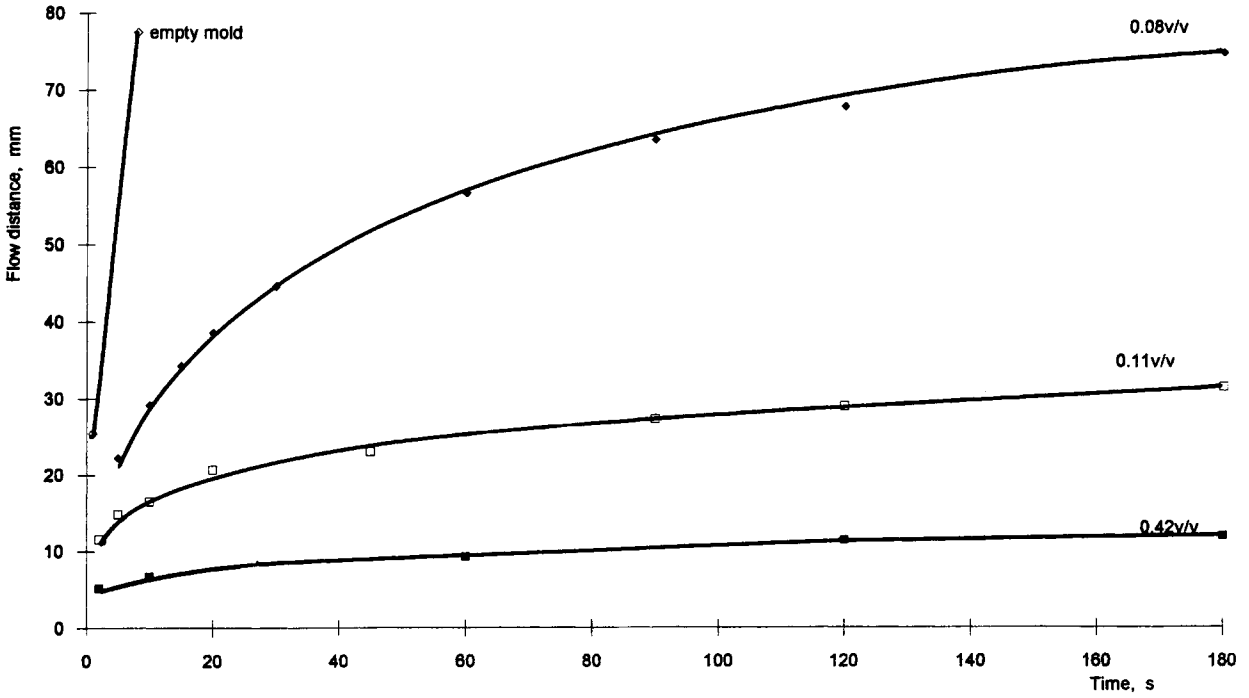

Figure 13 Flow rate for different fiber volume fractions; 1 bar; 1.7 dtex PET.

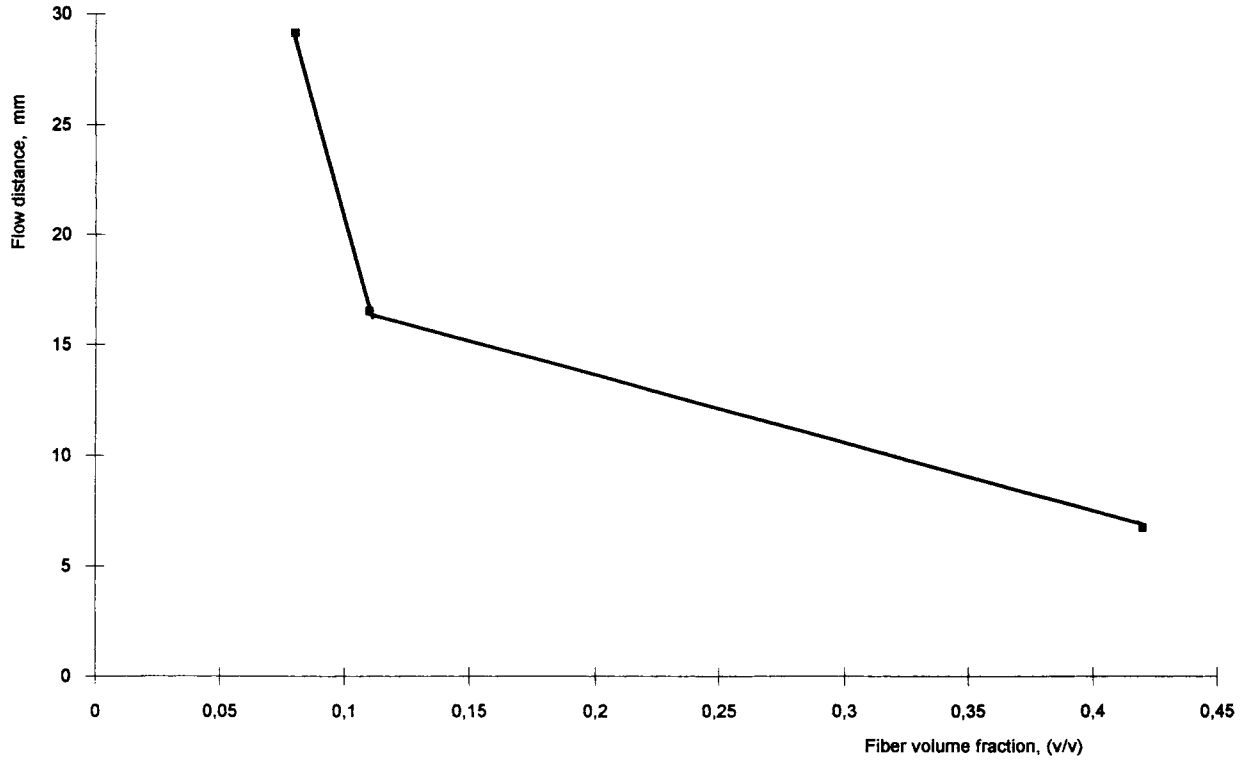

Figure 14 Effect of fiber volume fraction on flow distance; 2.6 bar; 1.7 dtex PET 10 s after injection start.

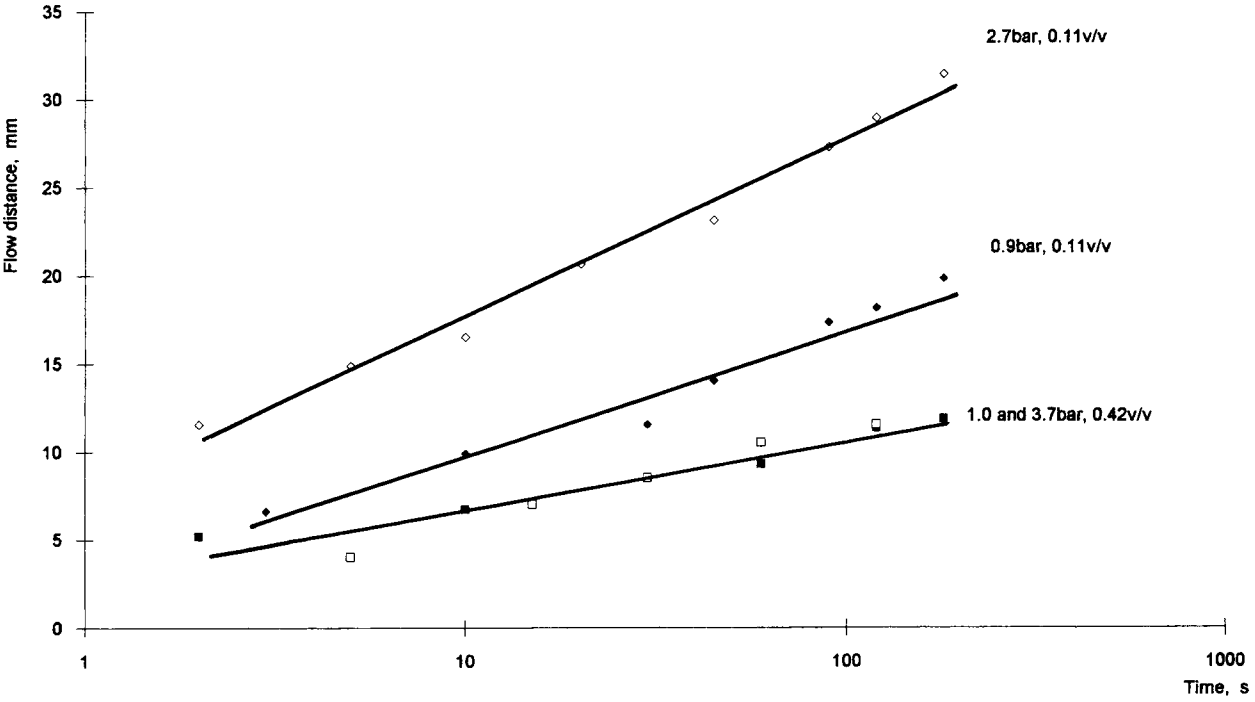

Figure 15 Flow distance vs. logarithm of time for different fiber volume fractions and pressures; 1.7 dtex PET (re Fig. 14).

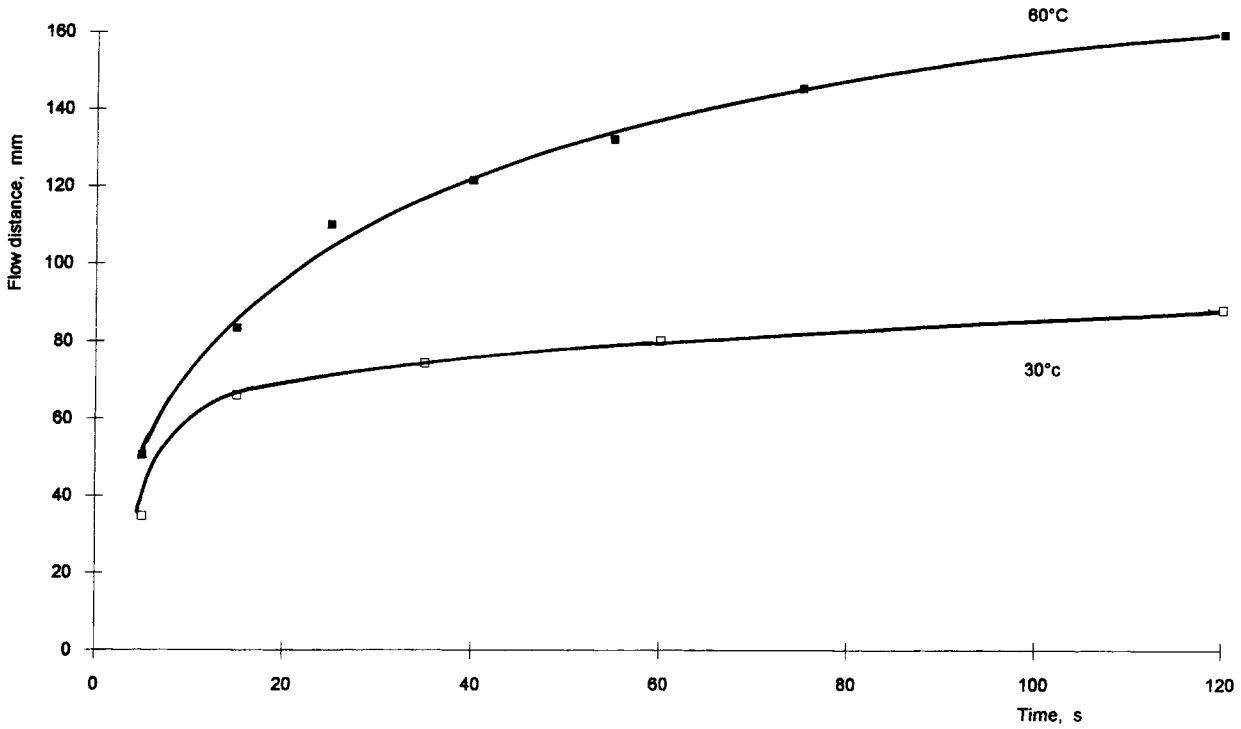

Figure 16 Rate of matrix flow at two different temperatures; 1.1 dtex PET; 2.6 bar; volume fraction 0.06.

eq. (6) correlated well with the values of the level of compression. Figure 20 shows the plot of permeability values as function of level of compression for mats consisting of 1.1 and 1.7 dtex polyester fibers. As can be seen from the figure, there is practically no difference between the two fiber types. The level of the permeability values is somewhat lower than the values for the spun-bonded and glass fiber mats reported by other workers,[11] thus indicating that the mats used in the present experiments have less open space between the fibers. Because eq. (5) is based on Darcy's law, the calculations indicate that the flow follows Darcy's law at least during the greatest part of the flow distance. Since the calculations were made using equations that are applicable only to Newtonian fluids, the results may indicate that the flow in the present experiments took place during the time when the polymer fluid was in its Newtonian stage. When eqs. (7) and (8) were used to calculate the time for the polymer to fill the mold, for both polyester and polyethylene fiber mats, very poor correlation was obtained; the experimentally measured flow rates were several orders of magnitude below the calculated ones. This disagreement may be due to increase in the level of compression of the fiber mat at or shortly prior to the advancing polymer front due to dislocation of the mat, as described later.

Plots of the squared flow distance vs. flow time according to Greve and Soh,[12] assuming that the wetted area is proportional to the squared flow distance in the case of circular polymer spreading, produced straight lines during the first 20–40 s of poly-

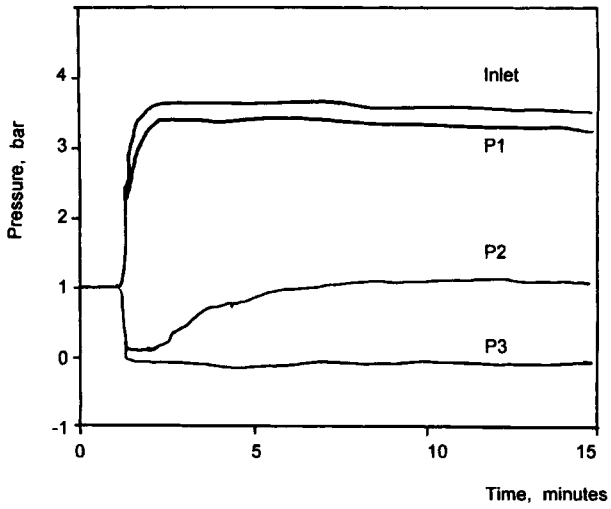

Figure 17 Pressures recorded at different points in the cavity during filling of the mold; curves correspond to locations starting from the polymer inlet in the following order: inlet, P1, P2, P3.

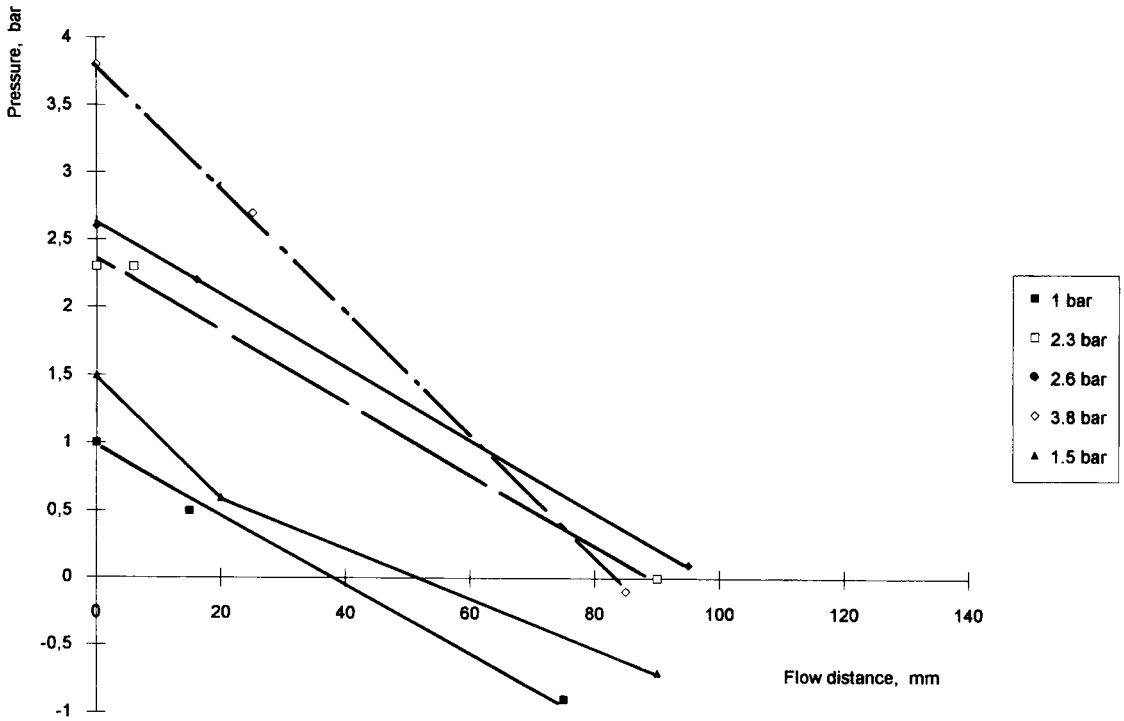

Figure 18 Plots of pressure as function of flow distance for several different initial pressures; 1.1 dtex PET; 25% level of compression.

mer flow. Then, the polymer flow slowed down in all cases. The time of linearity did not vary with injection pressure. This further indicates that the flow takes place in two sequences.

The marks of the tracing dyes indicated radial polymer flow from the inlet hole in the circular mold part; in the pertruding part, the flow was linear. Experiments with thermocouples and pressure trans-

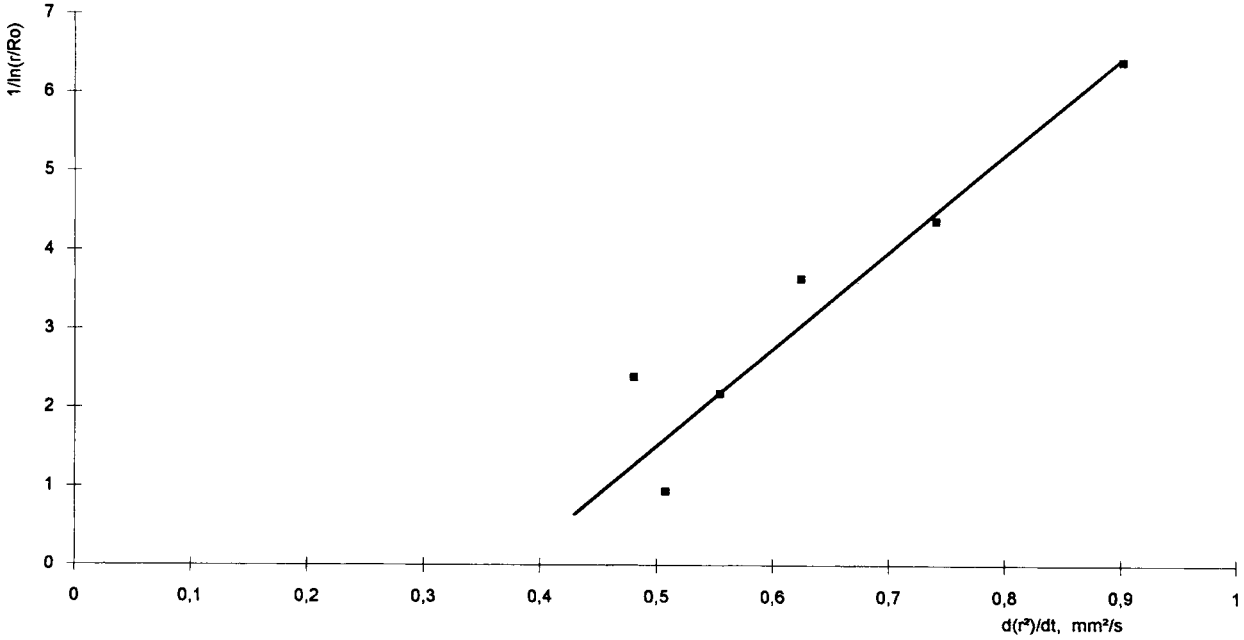

Figure 19 Plot of $1/\ln(r/R_0)$ vs. $d(r^2)/dt$ according to eq. (5); 4.4 dtex LLDPE; 50% level of compression.

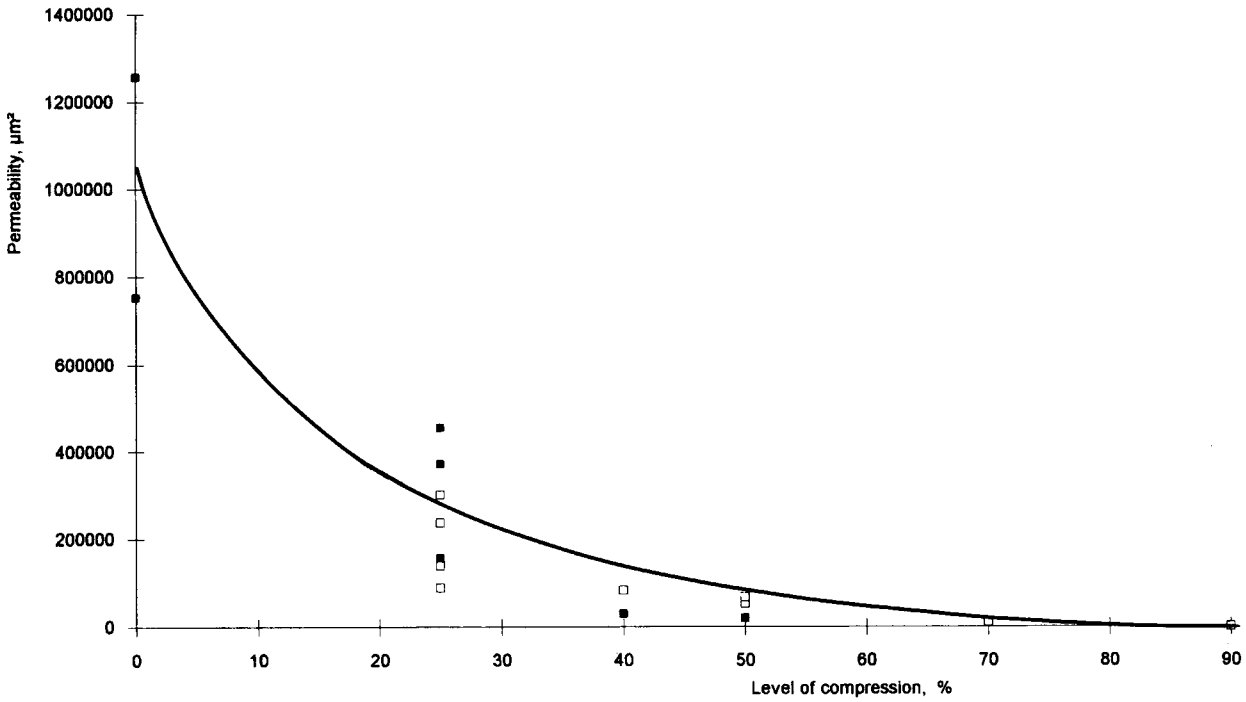

Figure 20 Permeability as function of level of compression; 1.1 and 1.7 dtex PET fiber mats.

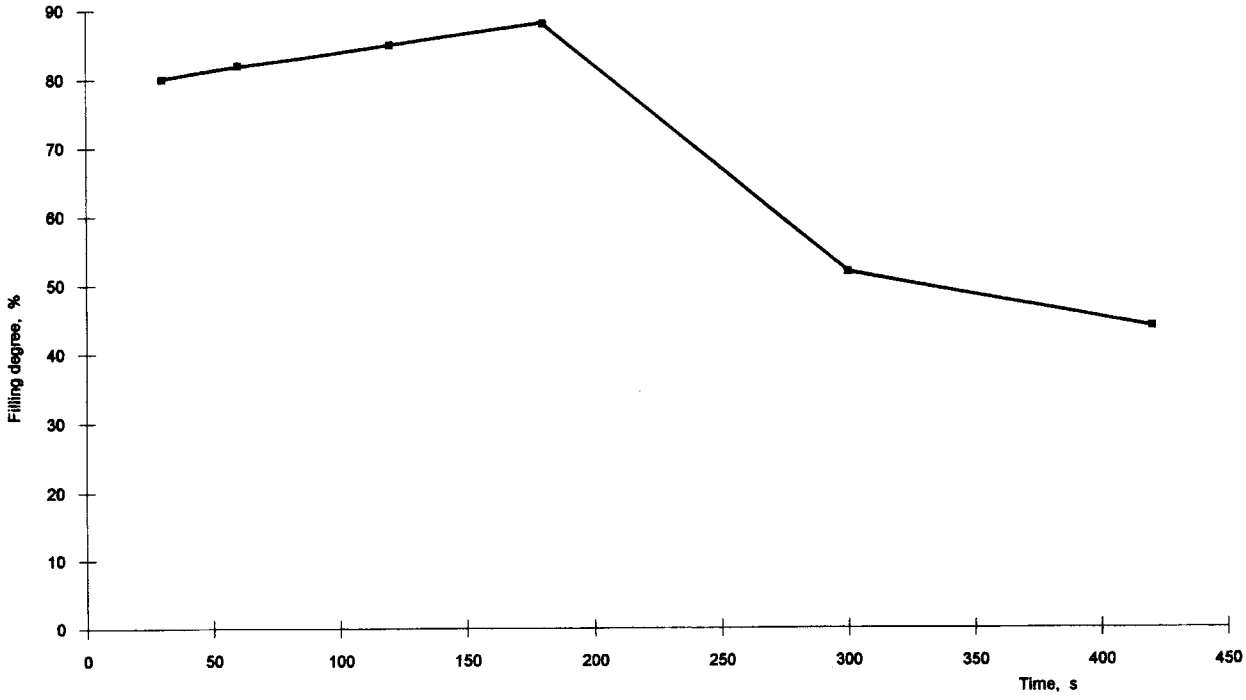

Figure 21 Effect of polyurethane matrix aging time on degree of filling; 2.6 bar; level of compression 25%, 1.1 dtex PET fibers.

ducers exhibited various degrees of disturbances in the flow patterns.

Dislocation of mat inside the cavity due to polymer flow during injection was observed in experiments with levels of compression of 25% and lower and for injection pressures from 2.6 bars upward. The process of dislocation accelerated considerably after the circular part of the cavity was completely filled. This supports findings reported earlier by the authors that a symmetrically situated injection hole helps to prevent dislocation of the mat.[6] When an unidirectional mat of 4.4 dtex LLDPE fiber was used, the mat was observed to stretch in the crosswise direction away from the polymer inlet hole well before the circular part was completely filled. This indicates that the polymer flow was responsible for dislocation of the mat in places where fiber–fiber bonding was not strong. The movement of the mat occurred predominately in parts already impregnated by the elastomer, which indicates that the fluid may have acted as a lubricant, lowering the friction between the mat and the wall of the cavity. The dislocation caused significant compression of the mat at or close to the advancing polymer front. The compression took place by movement of the mat in the direction of the plane of the flat cavity.

The degree of filling as function of aging time of the elastomer prior to the start of the polymer injection is shown in Figure 21, which shows that the degree of filling is lowered in the range 180–300 s. Cuts perpendicularly through the polymer matrix frontier as well as SEM photographs (Fig. 9) indicated that the flow was practically pluglike, i.e., the frontier was perpendicular to the outer surface of the sample.

CONCLUSIONS

Theoretical analysis were made of models for flow of elastimeric polymer fluid in fibrous structures. The validity of models was tested experimentally by investigating the flow of elastomeric polymer fluid in different fibrous structures in the SRIM process. The results are expected to contribute toward a better understanding of flow mechanisms in fibrous systems and, subsequently, result in better techniques for fabricating elastomer-based composites.

In experiments with SRIM molding, the flow rate of the elastomer fluid could be divided into two phases with two significantly different flow rates. The calculated values for the permeability of nonwoven mats were found to lie within the range of permeability values reported by other workers for spun-bonded nonwoven mats. The polymer flow in the present experiments took place during the time when the polymer fluid was in its Newtonian stage.

An obvious conclusion from calculations and experimental flow rate measurements would be that the elastomer flow in the SRIM molding first follows the law of Darcy and later continues as a capillary flow. This may further be supported by the fact that small menisci could be seen around fiber ends sticking out from a "frozen" portion of the polymer front. Against the conclusion regarding the capillary nature of the slow-flow phase weighs the fact that no wicking was noted when using elastomer as the test fluid in a wicking experiment.

The absorption rate of water obtained in experiments with wicking in the in-plane direction could be divided into two phases. One can conclude that even if the curves for the polymer flow rate and the wicking rate look similar the flow mechanisms are different: The wicking takes place only as a capillary flow, and the polymer flow apparently follows Darcy's law and eventually changes to capillary flow toward the end of the flow process.

Dislocation of the fiber mat during SRIM molding, which can cause significant changes in the level of compression in the mat, may occur when the point of polymer feeding is situated nonsymmetrically with respect to the contour of the mold. The fiber structure is more susceptible to local stretching in the directions where the cohesion between fibers is weaker, i.e., in the cross-fiber direction of unidirectionally laid fibers. An increased level of compression of the fibrous structure at or close to the polymer front due to dislocation may be part of the reason for the poor fit of the experimental data with the flow model equation.

Also, for the elastomer matrix, the dependence of the flow rate on fluid viscosity and temperature, on fiber volume fraction, as well as on fiber direction proved to behave in the manner familiar to the SRIM field. Also, the relation between pressure and fiber volume fraction as well as the relation between pressure and distance to the polymer inlet hole were similar for the elastomer matrix as for other polymers in SRIM.

This work was done at the Laboratory for Plastics and Fibre Technology (formerly Textile Laboratory) of The Research Centre of Finland as part of their composites research program and partly at Chalmers Technical University under the guidance of Professor Roshan Shishoo of TEFO and Chalmers Technical University, Gothenburg, Sweden. I (M. E.) want to extend my gratitude to them

for making this work possible. Furthermore, I want to thank Mr. Markku Sysmälä for his efforts in building the apparatus needed for the fabrication of the samples and Mmes. Rauni Jokinen and Vuokko Rounioja for assisting in analysis work, all of the Laboratory for Plastics and Fibre Technology.

NOMENCLATURE

a_{sample}	total area of composite sample
a_s	area of mat sample
bw_{mat}	basis weight of mat
c_1	level of compression
d_f	diameter of fiber
h_m	thickness of sample under actual experimental conditions
h_s	thickness of mat sample.
K	permeability
K_r	permeability in the radial direction
K_x	permeability in x-direction
L	distance of polymer travel
p	pressure
p_0	pressure at polymer inlet
p_r	pressure at liquid front
r	distance radially
R_0	radius of inlet hole of mold or center hole of mat
t	time
v_x	velocity of polymer liquid in x-direction
w_{fib}	weight of fiber material
w_{ms}	weight of mat sample
w_{matrx}	weight of matrix material
w_{sample}	weight of sample
$(w/w)_{\text{fib}}$	ratio fiber/total composite weight-to-weight, referred to as fiber weight fraction
α	portion of total area of sample impregnated with matrix measured with template
γ	surface energy
Δp	pressure difference
ϵ	porosity or resin volume fraction
Θ	contact angle
μ	viscosity
ρ_f	specific weight of fiber material
ρ_{matrix}	specific weight of matrix material
ϕ	ratio fiber/total composite volume-to-volume

REFERENCES

1. Product information, Merkblatt, Baytec Reparturund Giesssmassen Bayer PU/Anwendungstechnik Elastomere, Leverkusen, Germany, July 1987.
2. Product brochure, Tuoteseloste G 300 Polyesterihartsi, Neste Chemicals, Kulloo, Finland (technical brochure).
3. SP 110 Epoxy laminating system UK1102887-7, Structurel Polymer Systems Ltd., Coves, UK (technical brochure).
4. L. A. Gottler, K. S. Shen, *Rubber Chem. and Technol.*, **556,** 619 (1983).
5. M. Epstein and R. L. Shishoo, *J. Appl. Polym. Sci.*, **44,** 263–277 (1992).
6. M. Epstein and R. L. Shishoo, *J. Appl. Polym. Sci.*, **45,** 1693–1704 (1992).
7. M. Epstein and R. L. Shishoo, *J. Appl. Polym. Sci.*, to appear.
8. C. W. Macosko, RIM, *Fundamentals of Reaction Injection Molding,* Hanseer, Munich, Vienna, New York, 1989.
9. Z. Tadmor and C. G. Gogos, *Principles of Polymer Processing,* Wiley, New York, 1979.
10. B. R. Gebart, *J. Compos. Mater.*, **26**(8), 1992.
11. D. E. Hirt, K. L. Adams, R. K. Prud'homme, and L. Rebenfeld, *J. Therm. Insulat.*, **10,** 153 (1987).
12. B. N. Greve and S. K. Soh, *Directional Permeability Measurement of Fiberglass Reinforcements,* SAE Special Publication no. 812, 1990, p. 101.
13. M. V. Bruschke and S. G. Advani, *Polym. Compos.*, **11**(6), 398 (1990).
14. M.-K. Um and W. I. Lee, *Polym. Eng. Sci.*, **31**(11), 765 (1991).
15. A. W. Chan and S.-T. Hwang, *Polym. Eng. Sci.*, **31**(15), 1149 (1991).
16. Trevira Spinnfaser für Nonwovens und voluminöse Vliese, Product information brochure, February 1991, Hoechst AG, Verkauf Fasern, Postf. 800320, D 6230 Frankfurt/Main 80, Germany (technical report).
17. LLDPE, telefax communication with Neste Oy, Porvoo, Finland (Olli T. Turunen), January 18, 1993.
18. *Dyneema SK 60 High Strength/High Modulus Fiber, Properties & Applications,* Dyneema Vof, Dr Nolenslaan 119A, P.O. Box 599, 6130 AN Sittard, The Netherlands (product information).
19. Instruction Manual, Baytec Reparatur- und Giessmassen, Bayer PU/Anwendungstechnik Elastomere, Leverkusen, Germany, 1987.
20. SFS-Käsikirja 27, Osa 1, 3 painos, lokakuu 1987, Suomen Standardoimisliitto, Helsinki, Finland, SFS3192, corresponds to ISO 3801:1977 Textiles. Determination of mass per unit area and per unit length for textile fabrics.
21. SFS-Käsikirja 27, Osa 1, 3 painos, lokakuu 1987, Suomen Standardoimisliitto, Helsinki, Finland, SFS 3380, corresponds to ISO 5084:1977 Textiles. Determination of thickness of textile fabrics.

Received May 26, 1993
Accepted September 8, 1993